ORIGINAL RESEARCH

Using Olink Proteomics to Identify Inflammatory Biomarkers in the Cerebrospinal Fluid in Guillain-Barré Syndrome

Shuanghong Sun, Meng Li*, Jihe Song*, Di Zhong

Department of Neurology, The First Hospital of Harbin Medical University, Harbin, Heilongjiang, People's Republic of China

*These authors contributed equally to this work

Correspondence: Di Zhong, Department of Neurology, The First Hospital of Harbin Medical University, Harbin, Heilongjiang, People's Republic of China, Email sjnkzhongdi@163.com

Purpose: The precise etiology of Guillain-Barré syndrome (GBS) is uncertain; however, it is linked to immunological and inflammatory processes. Thus, this research aims to investigate new inflammatory biomarkers for GBS diagnosis.

Patients and Methods: In this work, Olink proteomics was used to compare the expression levels of 92 inflammation-related proteins in the cerebrospinal fluid (CSF) of patients with non-inflammatory neurological diseases (n=14) and GBS (n=23). Differentially expressed proteins (DEPs) were then analyzed biologically and in terms of their relationship to clinical features, and logistic regression models were built. We also downloaded GEO data to validate DEPs at the mRNA level.

Results: We identified twenty DEPs. The PPI network screened six key DEPs (including TNF, CCL20, IL8, MCP-1, IL10, and IL5). These DEPs were enriched in the chemokine signaling pathway, the IL-17 signaling pathway, cytokines and their receptor interactions, and other pathways. TNFRSF9 and IL-10RB showed the strongest correlation of expression in CSF. CCL20 and IL5 could be used as potential independent predictors for the diagnosis of GBS. Seven DEPs (MCP-1, CXCL1, MCP-4, MMP-10, CXCL10, CCL28, and CCL20) had some predictive value for the severity of GBS. Based on the validation of the GEO data, the mRNA expression of MCP-1 and CXCL9 was found to be upregulated at the peak of EAN, and the enriched pathways at the gene transcription level were consistent with the results of this study.

Conclusion: DEPs linked to inflammation (such as TNF, CCL20, IL8, MCP-1, IL10, and IL5) could be useful biomarkers for GBS diagnosis. More research is required to determine their precise mechanisms in GBS.

Keywords: Guillain-Barré syndrome, inflammation, biomarkers, olink proteomics, bioinformatics analysis

Introduction

The most frequent cause of acute flaccid paralysis worldwide is Guillain-Barré Syndrome (GBS),[1] characterized by symmetrical ascending muscle weakness, reduced tendon reflexes, and different degrees of sensory involvement. Between 0.81 and 1.91 cases of GBS are reported for every 100,000 people annually.[2] Men are more likely than women to develop the condition, with an incidence that rises by 20% for every ten years of age. Between 3% and 7% of people die from the condition, and up to 20% of people lose their ability to walk on their own six months after the illness first manifests.[3,4] Though the exact cause of GBS is unknown, it is currently thought to be an autoimmune-mediated peripheral neuropathy. This process is brought on by molecular mimicry between gangliosides on the membranes of microorganisms and peripheral nerve cells,[5] which activates the complement and macrophage systems, T cell-mediated cytotoxicity, and other immune responses that cause demyelination and axonal damage in the peripheral nervous system, respectively, and ultimately advances the disease.[6] The two most popular immunotherapies for treating GBS are plasma exchange and intravenous immunoglobulin.[7] In principle, immunotherapy should be started as soon as possible before

Graphical Abstract
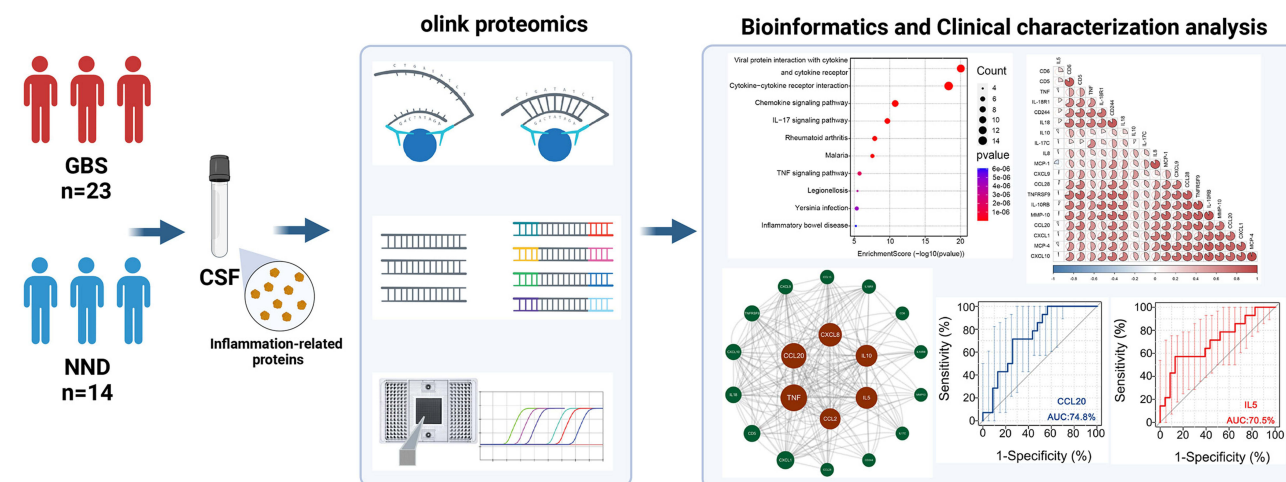
irreversible neurological damage occurs. Still, because there are multiple subtypes and variants of GBS, there are no specific diagnostic biomarkers and a lack of targeted therapeutic interventions.[8]

Many biomarkers have been linked to GBS in recent years. These include decreased levels of TGOLN2 and NCAM1 and increased levels of APOC3 in the CSF of GBS patients compared to patients with noninflammatory neurological disease(NND),[9] and serum C3 complement levels as a predictor of the prognosis of GBS and for tracking disease activity.[10] In Guillain-Barre syndrome, Thomma et al discovered that high and sustained anti-GM1 antibody titers were linked to a poor prognosis.[11] Although these biomarkers have been linked to GBS, the diagnosis has limits. Few of these biomarkers are being used clinically.[12] Thus, searching for new GBS biomarkers is vital to learning more about the disease's etiology, providing early and precise diagnosis, and enhancing patient outcomes.

Olink proteomics is the accurate detection of proteins based on the highly sensitive, particular, and excellently scalable proximity extension assay.[13,14] This development has dramatically aided in identifying novel biomarkers for prognosis and disease prediction and improved comprehension of the molecular mechanisms of pathogenesis and the distinctive signaling networks associated with particular diseases.[15] In this paper, we analyzed the expression levels of CSF inflammation-related proteins in patients with GBS at the peak of the disease and in control patients using Olink proteomics technology. Additionally, logistic regression model building and bioinformatic analysis were carried out. To study the biomarkers of GBS cerebrospinal fluid to explore the role of immune inflammation in developing GBS and related mechanisms and to provide a theoretical basis for the diagnosis and targeted therapy of GBS.

Materials and Methods
Patient Selection and Clinical Data Collection
The experimental group consisted of twenty-three GBS patients hospitalized at the First Hospital of Harbin Medical University between January 2021 and December 2022. In contrast, the control group consisted of fourteen patients with NND. All patients in the experimental group were at the peak of the illness and satisfied the diagnostic requirements for Guillain-Barré syndrome.[16] Exclusion of patients with infection, fever, and immunomodulatory therapy before baseline sampling. Clinical information about the patients was documented, such as their sex, age, duration of hospitalization, clinical signs and symptoms, blood counts, results from the CSF, and Hughes Functional Classification Scale score at the height of the illness.[17,18] Every patient enrolled in the study signed an informed consent form, which was carried out in compliance with the principles of the Declaration of Helsinki. The First Hospital Ethics Committee of Harbin Medical University approved this study (No. 2019115).

Collection of CSF Specimens

All recruited patients had 2 mL of CSF extracted at their initial lumbar puncture following hospital admission, which was then kept in a refrigerator at −80°C.

Proteomics Analysis

A proximity extension assay from Olink, which analyzes 92 inflammation-related biomarkers simultaneously, was used to analyze CSF samples.[19] In short, two antibody probes labeled with oligonucleotides attached to a target protein. The oligonucleotides then hybridize in pairs when the two probes are close. DNA polymerase is added, and this causes a DNA polymerization reaction that yields a distinct PCR target sequence. A microfluidic real-time PCR device (Signature Q100, OLINK) is then used to identify and measure the resultant DNA sequence. Following quality control and normalization of the resultant Ct data using a series of internal and external controls, the assay readings are reported as Normalized Protein Expression (NPX) values, where higher values correspond to higher protein expression levels.[20,21]

Bioinformatics Analysis

The protein expression levels in the two groups were compared differently in the Olink data results, and the Benjamini-Hochberg method was used to adjust for multiple comparisons. Following screening correction, proteins were classified as differentially expressed proteins (DEPs) if their p-value was less than 0.05. DEPs were visualized in the R program using the ggplot2 package, pheatmap package, etc. The discovered DEPs were subjected to pathway enrichment studies by the Kyoto Encyclopedia of Genes and Genomes (KEGG) and Gene Ontology (GO),[22,23] with p values < 0.05 and q values < 0.05. In both the experimental and control groups, all 92 inflammation-associated biomarkers were subjected to Gene Set Enrichment Analysis (GSEA).[24] Using DEPs as query proteins and Cytoscape for visualization, the STRING database (http://string-db.org) was used to evaluate protein-protein interactions (PPI) in functional protein binding networks.[25] We used the cytoNCA topology analysis plugin to screen for key differentially expressed proteins using the Betweenness Centrality (BC) algorithm.[26]

Construction of Logistic Regression Models

Using SPSS 25.0 software, the R software rms package, the pROC package, and the multipleROC tool, we ran a one-way logistic regression analysis on 20 CSF DEPs. After the proteins were screened using the single-factor logistic regression analysis, they were subjected to a regression analysis using the least absolute shrinkage and selection operator (LASSO) in R software. This method was used to select features and confirm the appropriate tuning parameter (λ) for the LASSO logistic regression. Cross-validation was also employed. Finally, multifactorial stepwise logistic regression analysis was incorporated to apply statistically significant predictors, construct a predictive model, and plot risk column lines.[27,28] The receiver operating characteristic (ROC) curve was used to evaluate the diagnostic performance of the DEPs, and the area under the curve (AUC) was computed.[29]

GEO Data Validation

The Gene Expression Omnibus (GEO) database (http://www.ncbi.nlm.nih.gov/geo) provided us with the GSE133750 dataset. This dataset represents a transcriptome sequencing of the sciatic nerve in a rat animal model of GBS called experimental autoimmune neuritis (EAN). We then used the R software's DESeq2 package to estimate the levels of gene expression and identified differentially expressed genes (DEGs) based on peak EAN and control-adjusted p-values < 0.05 and |log2 fold change| ≥ 1, as well as DEGs. We used the ggplot2 package to visualize volcano plots. After finding the intersection of DEGs and DEPs, we analyzed the discovered DEGs for GO and KEGG pathway enrichment using the R software Venn diagram package and ggplot2 package to create Wayne diagrams.

Statistical Analysis

Software such as SPSS (version 25.0), GraphPad (version 8.0.2), R (version 4.3.0), and Cytoscape (version 3.9.1) were used for statistical data analysis. Data are provided as mean ± standard deviation (normal distribution) or median (P25,

P75). The Wilcoxon rank sum test or the two-tailed independent samples *t*-test was used to compare the mean differences between the two groups. Pearson or Spearman conducted correlation analysis. Statistics were deemed significant if *P*<0.05.

Results

Clinical Characteristics of Patients in the GBS and NND Groups

This study comprised 37 samples, including 14 patients with NND and 23 with GBS. The general clinical characteristics of all subjects are shown in Table 1.

Screening for Differentially Expressed Proteins in CSF

Details of the Olink proteomics technology's identification of 92 inflammation-associated proteins are provided in Table S1. We screened 20 differentially expressed proteins associated with the development of GBS compared to control patients. The majority of these belonged to the chemokine and cytokine groups (Table S2). One protein (IL5) had its expression downregulated, whereas 19 other proteins (IL8, CD244, IL-17C, MCP-1, CXCL9, CXCL1, CD6, IL18, MCP-4, IL-10RB, IL-18R1, MMP-10, IL10, TNF, CD5, CXCL10, CCL28, TNFRSF9, and CCL20) had their expression raised (Figure 1A). Two clusters with distinct accumulation patterns were visible in the heatmaps of all 20 DEPs (Figure 1B), and Figure 1C displays the differences in protein expression between the GBS and NND groups.

Table 1 Clinical Characteristics of the Study Population

Variable	Overall, N = 37	NND, N = 14	GBS, N = 23	P value
Sex				0.031
Male	19 (51%)	4 (29%)	15 (65%)	
Female	18 (49%)	10 (71%)	8 (35%)	
Age	51 (38, 59)	49 (38, 56)	51 (38, 62)	0.6
Days of hospitalization	8 (6, 11)	6 (4, 7)	10 (8, 12)	<0.001
WBC (10^9/L)	6.74 (5.71, 8.37)	6.47 (5.39, 7.47)	6.94 (5.91, 9.04)	0.2
NEUT%	65 (60, 75)	62 (60, 71)	71 (58, 76)	0.5
NEUT# (10^9/L)	4.48 (3.45, 6.08)	3.91 (3.30, 5.18)	5.38 (3.64, 6.88)	0.2
LYMPH%	25 (17, 33)	30 (23, 33)	19 (17, 32)	0.3
LYMPH# (10^9/L)	1.70 (1.27, 2.16)	1.62 (1.23, 1.99)	1.82 (1.45, 2.18)	0.8
MONO%	5.85 (4.57, 6.93)	5.70 (4.07, 6.18)	6.30 (4.94, 8.53)	0.14
MONO# (10^9/L)	0.39 (0.30, 0.53)	0.33 (0.23, 0.40)	0.48 (0.35, 0.65)	0.012
PLT (10^9/L)	248 (216, 286)	238 (196, 272)	254 (221, 287)	0.4
NLR	2.61 (1.82, 4.30)	2.10 (1.83, 3.06)	3.69 (1.86, 4.42)	0.3
PLR	147 (129, 183)	151 (140, 170)	140 (124, 187)	>0.9
MLR	0.23 (0.17, 0.34)	0.19(0.17, 0.24)	0.27 (0.18, 0.38)	0.049
SII	666 (442, 1054)	608 (425, 769)	961 (486, 1130)	0.2
SIRI	1.00 (0.60, 1.99)	0.86 (0.48, 1.05)	1.54 (0.63, 2.37)	0.071
CSF total protein (mg/L)	410 (276, 676)	264 (240, 355)	574 (420, 1261)	<0.001
CSF IgG (mg/L)	37 (22, 62)	22 (20, 28)	53 (38, 154)	<0.001
CSF IgM (mg/L)	0.5 (0.3, 2.9)	0.3 (0.2, 0.3)	1.3 (0.5, 7.4)	<0.001
ALB (g/L)	38.2 (36.1, 40.5)	37.0 (36.0, 38.0)	38.5 (36.2, 40.8)	0.3
Serum sodium (mmol/L)	142.7 (139.8, 146.9)	147.1 (145.4, 149.0)	140.9(137.6, 142.6)	<0.001

Abbreviations: GBS, Guillain-Barré syndrome; NND, noninflammatory neurological disease; WBC, white blood cell; NEUT%, neutrophil percentage; NEUT#, absolute neutrophil value; LYMPH%, lymphocyte percentage; LYMPH#, absolute lymphocyte value; MONO%, monocyte percentage; MONO#, absolute monocyte value; PLT, platelet; NLR, neutrophil-to-lymphocyte ratio; PLR, platelet-to-lymphocyte ratio; MLR, monocyte to lymphocyte ratio; SII, systemic immune inflammation index; SIRI, systemic inflammation response index; CSF, Cerebrospinal fluid; ALB, Albumin.
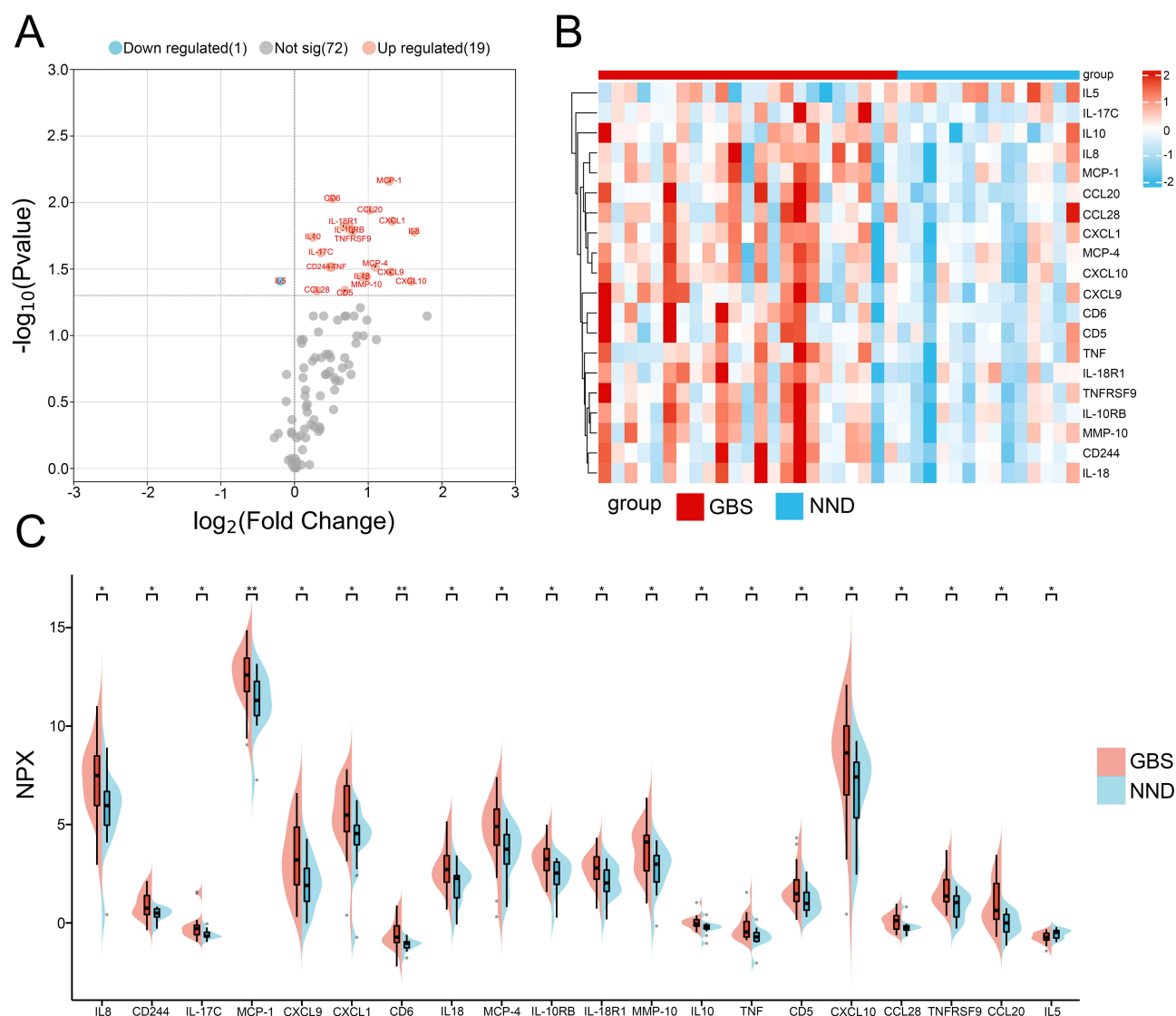
Figure 1 Inflammation-related protein alterations were noted in both the NND and GBS groups. (**A**) Visualization of 92 biomarkers associated with inflammation using volcano plots. Proteins with significant differential expression are indicated by gray nodes; down-regulated proteins are indicated by blue nodes; and up-regulated proteins are indicated by red nodes. (**B**) The heatmap shows proteins linked to inflammation that are differentially expressed; red indicates high expression, and blue indicates low expression. Each row in the map represents a protein, and each column represents a sample. (**C**) A pod plot showing how 20 DEPs are expressed. *P<0.05; **P<0.01.

Bioinformatic Analysis of DEPs Associated with GBS Inflammation

We used GO and KEGG enrichment analysis to investigate the role of CSF DEPs in GBS in more detail. Cell chemotaxis, cellular response to LPS, cytokine activity, and other phrases were among the enriched GO terms displayed in Figure 2. Cytokine-cytokine receptor interactions, viral proteins interacting with cytokines and cytokine receptors, chemokine signaling routes, IL-17 signaling pathways, TNF signaling pathways, and other pathways implicated in GBS pathogenesis were identified by KEGG enrichment analysis (Figure 3A). We also conducted GSEA analysis to investigate the signaling pathways enriched by the gene collection of CSF proteins from GBS patients (Figure 3B). These proteins were implicated in JAK-STAT signaling pathways, cytokine-cytokine receptor interactions, and chemokine signaling pathways in this investigation. To vividly illustrate the connections between the proteins, we built a PPI network, as seen in Figure 3C. Six proteins were identified as important nodes in the PPI network, including TNF, CCL20, IL8, MCP-1, IL10, and IL5. This implies that they might have significant functions in GBS and could be useful biological indicators for GBS prediction.
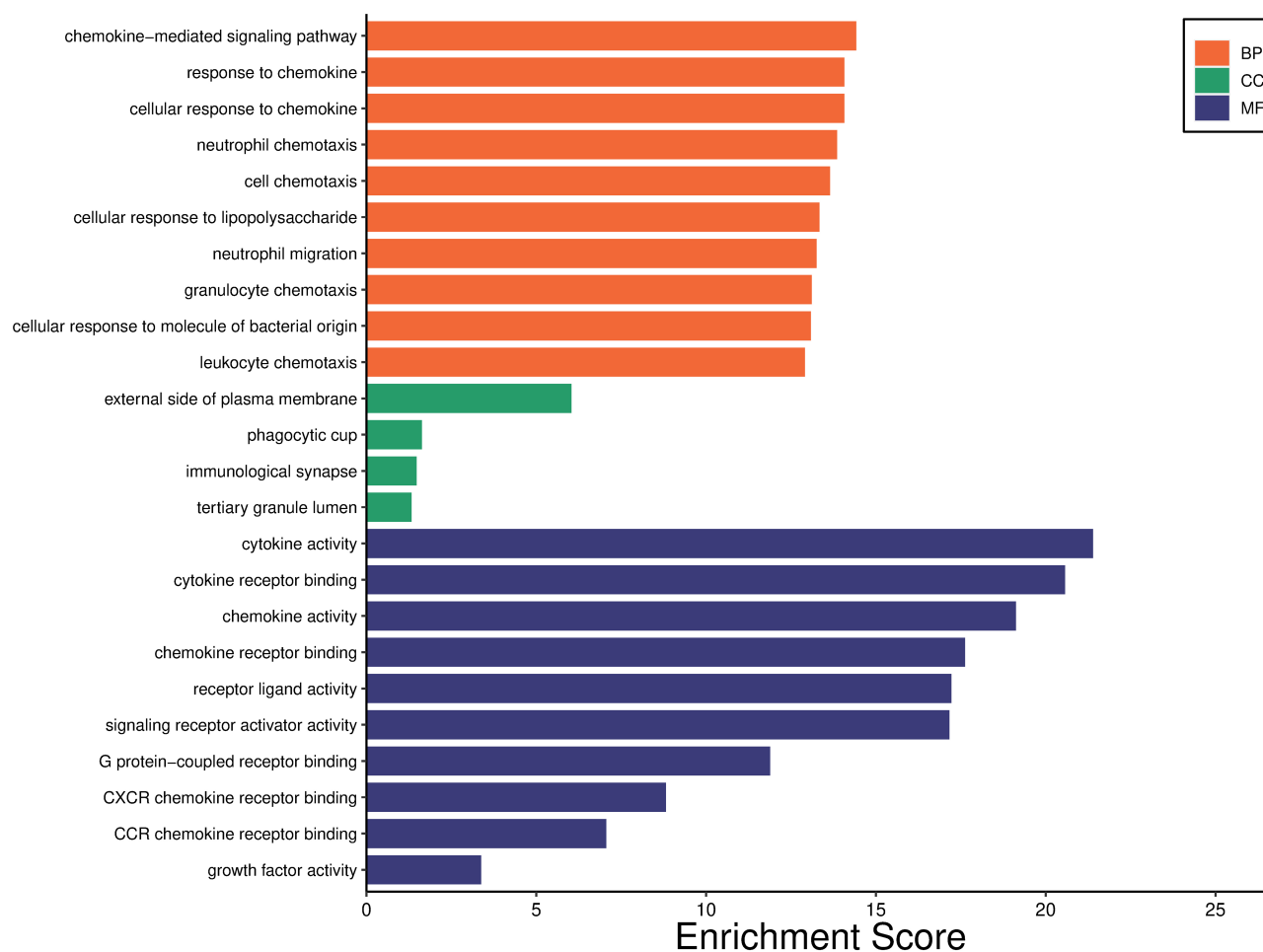
Figure 2 Analysis of DEPs' GO enrichment. Bar graphs depict the molecular functions (MF), biological processes (BP), and cellular component biological processes (CC) connected to the proteins with differential expression.

Correlation Analysis Between Differentially Expressed Inflammatory Proteins

We further analyzed the correlation between DEPs in the CSF (Figure 4A). IL8 and MCP-1 (R = 0.812, $P = 2.51\times10^{-6}$), MCP-1 and CCL20 (R = 0.747, $P = 4.21\times10^{-5}$), CCL20 and IL8 (R = 0.726, $P = 8.71\times10^{-5}$), and CXCL10 and MCP-4 (R = 0.907, $P = 2.41\times10^{-9}$) were found to have high associations. This finding suggests the possibility of a synergistic expression profile across members of the chemokine family. The strongest connection in CSF was seen between TNFRSF9 and IL-10RB (R = 0.946, $P = 1.03\times10^{-11}$), and scatter plots were created using this information (Figure 4B). This may reflect the dynamic balance between pro-inflammatory (TNF) and anti-inflammatory (IL10) pathways during the acute phase of GBS.

Correlation Analysis of DEPs with Clinical Features

As seen in Figure 4C, the relationships between each CSF protein and clinical characteristics were evaluated. CCL20 (R = 0.46, P = 0.037) demonstrated a positive correlation with hospitalization days, indicating that it might be a reflection of the course of the disease. Monocyte percentage, CXCL9 (R = 0.53, P = 0.014), and IL5 (R = 0.45, P = 0.031) showed a pattern of correlation, which could indicate monocyte-macrophage system activation. IL10 and CSF IgM were shown to be positively correlated (R = 0.47, P = 0.027). The three proteins that showed a positive connection with the Hughes score were MCP-4 (R = 0.48, P = 0.019), CXCL10 (R = 0.42, P = 0.042), and CCL28 (R = 0.47, P = 0.024). This implies that they may serve as indicators of the severity of the condition.
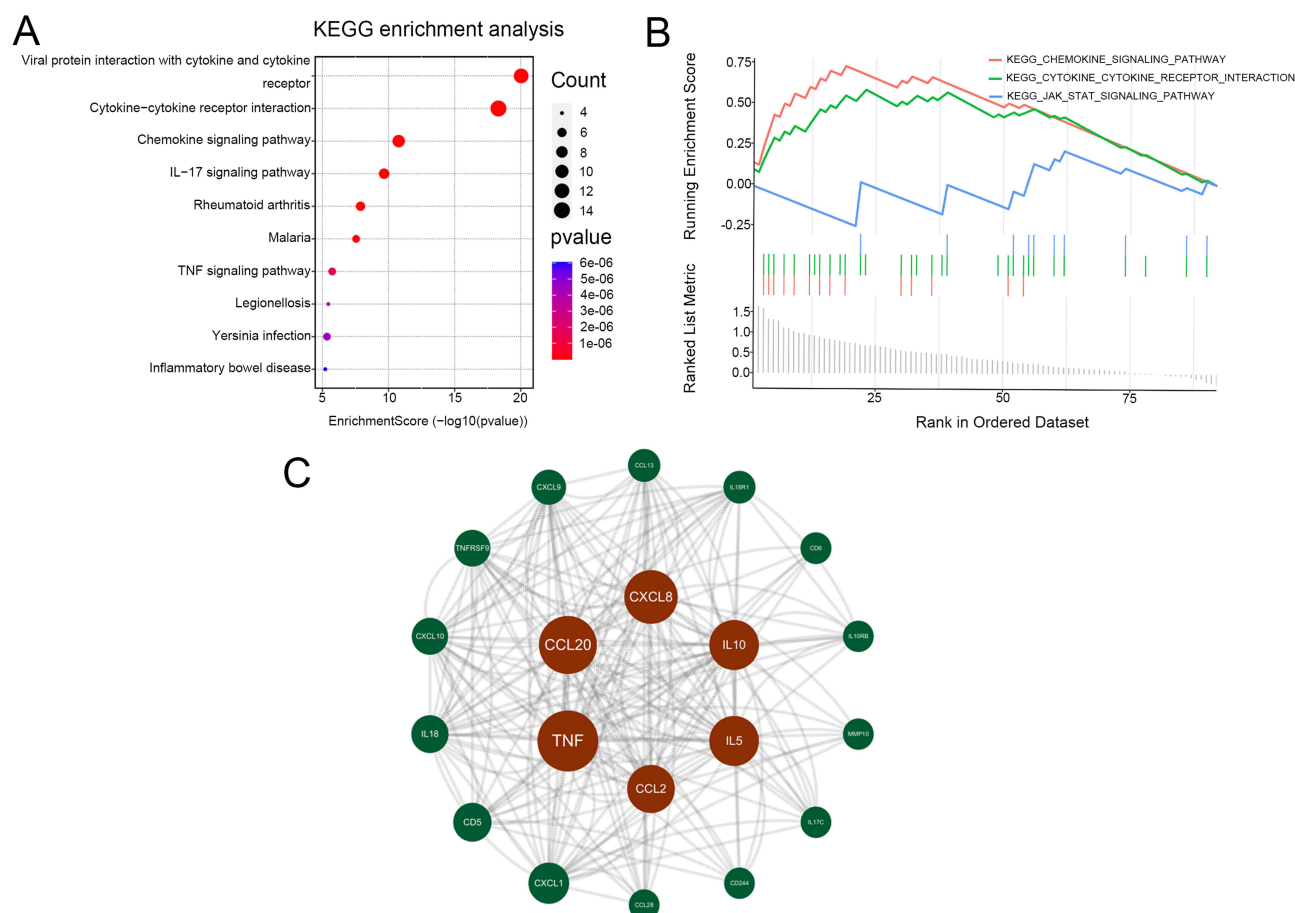
Figure 3 KEGG analysis, GSEA analysis, and PPI network. (**A**) The bubble graph displays the top 10 enriched pathways from the KEGG enrichment analysis. The horizontal coordinates represent the number of genes or total number of genes enriched in KEGG pathways. The size and color of the dots on the graph correspond to the number of genes and the magnitude of the p-value, respectively. (**B**) Gene set enrichment analysis (GSEA) outcomes using 92 proteins linked to inflammation as the background. (**C**) PPI network analysis of differentially expressed proteins associated with inflammation.

Constructing Logistic Regression Models

We created one-way logistic regression models for every protein in the CSF of GBS patients to assess the diagnostic potential of 20 DEPs, and we then displayed forest plots (Figure 5A). Sixteen potential proteins were initially identified as IL8, CD244, MCP-1, CXCL9, CXCL1, CD6, IL18, IL-10RB, IL-18R1, MMP-10, IL10, TNF, CCL28, TNFRSF9, CCL20, and IL5.

The best predictors of the current risk variables were chosen by using the LASSO regression approach to the proteins tested in the one-way logistic regression analysis, as illustrated in Figure 5B and C. Six prospective predictors with non-zero coefficients were ultimately chosen from among the 16 pertinent variables: CXCL9, CD6, IL10, TNF, CCL20, and IL5.

Multifactorial logistic stepwise regression analysis was then used to introduce the features selected in the LASSO regression model and construct a predictive model to identify potential biomarkers. Among these, CCL20 and IL5 showed statistically significant differences and were plotted accordingly in the GBS risk nomogram (Figure 5D). This implies that IL5 downregulation and CCL20 overexpression may work together to predict GBS. An AUC of 0.748 for CCL20 (Figure 5E) and 0.705 for IL5 (Figure 5F) were obtained by ROC analysis. CCL20 and IL5 together had a better diagnostic capacity than either indicator alone (AUC of 0.807) (Figure 5G).

Predictive Value of DEPs for GBS Disease Severity

A mild group (Hughes ≤3 points, n = 16) and a severe group (Hughes >3 points, n = 7) were separated from the GBS patients in order to evaluate the relationship between CSF DEPs and the severity of GBS. We created a forest plot and
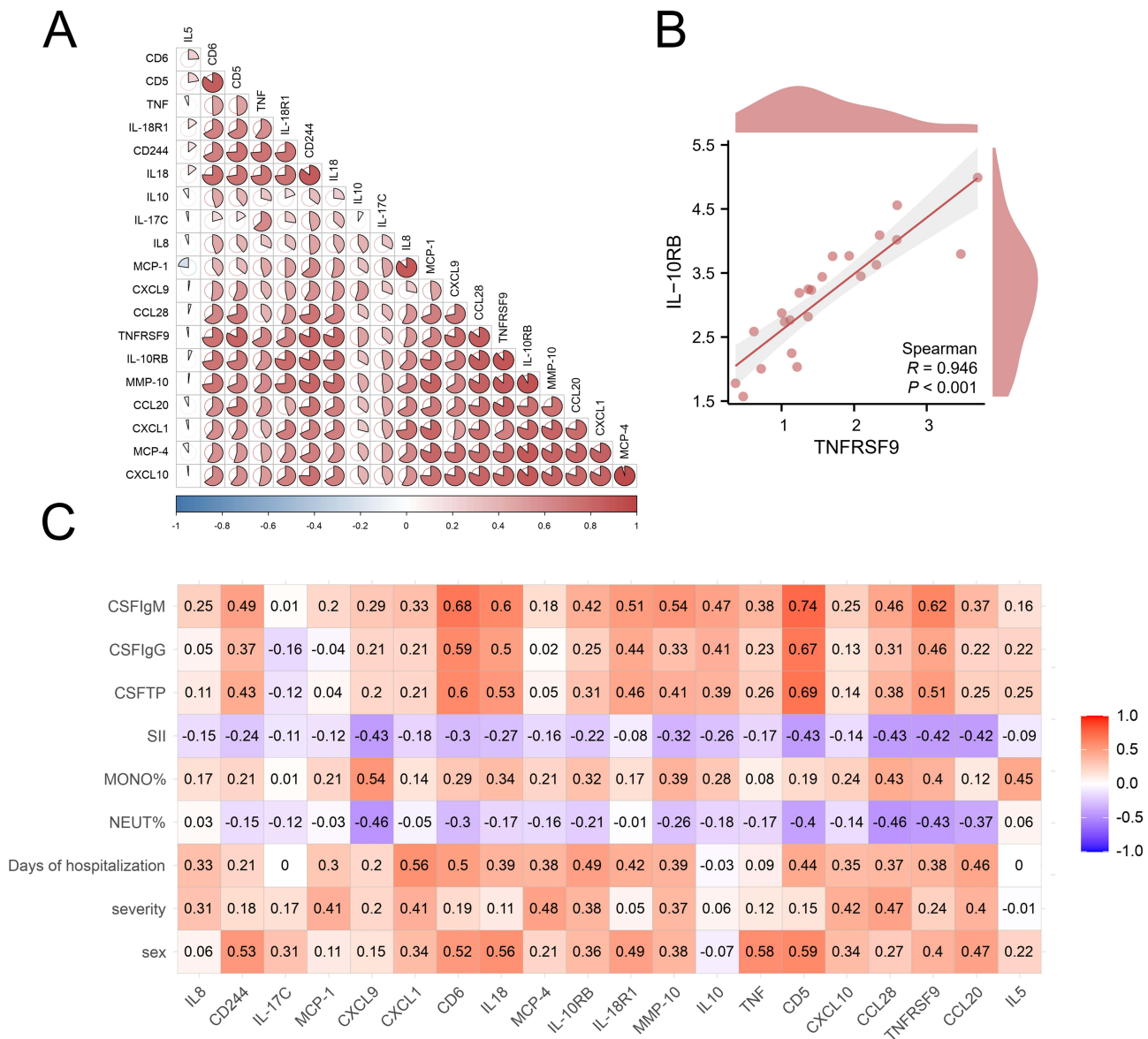
Figure 4 Investigation of the correlation between clinical characteristics and DEPs. (**A**) Analysis of correlations between inflammatory biomarkers that are differentially expressed in Guillain-Barré syndrome patients. The pie chart in each cell indicates the amount of the correlation coefficient. (**B**) Scatter plot demonstrating the TNFRSF9 and IL-10RB positive connection that is most significant. (R=0.946, P=1.03×10^{-11}), where the Spearman correlation coefficient is represented. (**C**) A heatmap showing the relationship between nine clinical characteristics and 20 inflammation-associated differentially expressed proteins (DEPs). The Spearman correlation coefficient, represented by the number in each cell, shows the correlation coefficient's magnitude.

conducted a one-way logistic regression analysis (Figure 6A). The results showed that MCP-4 and CCL28 were significantly correlated with disease severity and could be used as potential predictors for the diagnosis of severe GBS. The AUC values of seven proteins (MCP-1, CXCL1, MCP-4, MMP-10, CXCL10, CCL28, and CCL20) were found to be >0.7 when the predictive power of DEPs for severe GBS was examined using ROC curves (Figure 6C). Of them, MCP-4's diagnostic value (AUC=0.804) outperformed the other six DEPs. With an AUC of 0.857, the seven DEPs indicated severe GBS (Figure 6B). However, more functional studies are required to confirm if these markers directly influence the course of the disease.

## Validation of DEPs at mRNA Level Using GEO Data

We acquired the sciatic nerve transcriptome data of the EAN rat model from the GEO database (GSE133750) in order to confirm the accuracy of the proteomics findings. Rats' peripheral nerve tissues during the peak of EAN showed
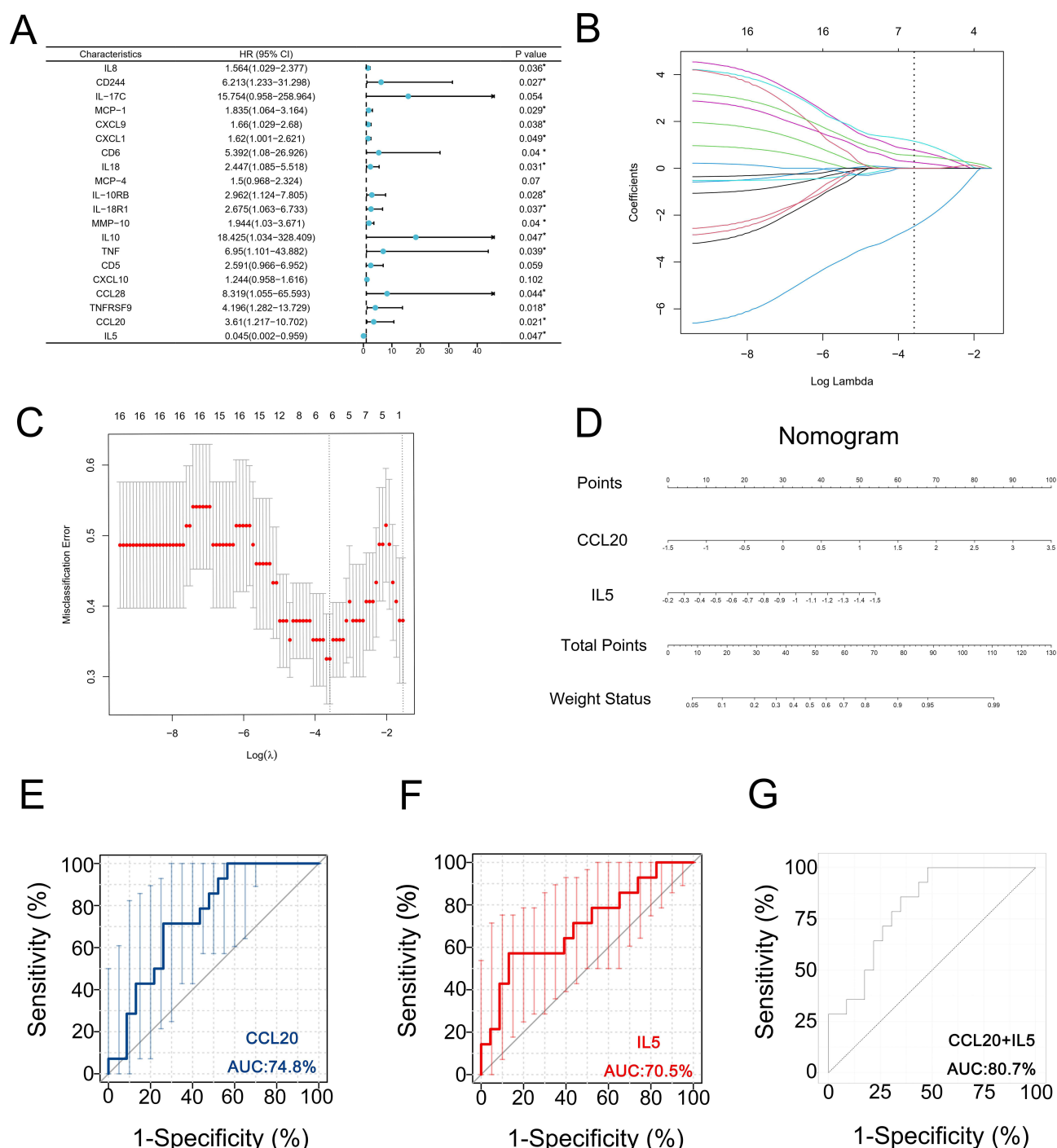
Figure 5 Models for logistic regression were built. (**A**) Forest plot of a one-way logistic regression analysis comparing the GBS group to the control group. Variable selection for the binary logistic regression model LASSO (**B** and **C**). The log (lambda) series was used to plot the coefficients. Based on ideal lambda values, six variables with non-zero coefficients were chosen. After verifying that lambda is the optimal parameter in the LASSO model, partial likelihood deviation (binomial deviation) curves were plotted against log (lambda), and dashed vertical lines were plotted according to the one standard error threshold. (**D**) Column plots of risk containing IL5 and CCL20 as predictors. (**E**) ROC curves for the GBS CCL20 diagnostic. (**F**) ROC curve for the GBS IL5 diagnostic. (**G**) CCL20+IL5 ROC curve for combined GBS diagnosis. *P<0.05.

significantly different mRNA expression from controls, according to statistical analysis. A volcano plot was created, showing 126 genes with up-regulated expression and 11 with down-regulated expression (Figure 7A). A Venn diagram was created by intersecting the 137 DEGs in EAN with the 20 DEPs in GBS (Figure 7B). The findings demonstrated
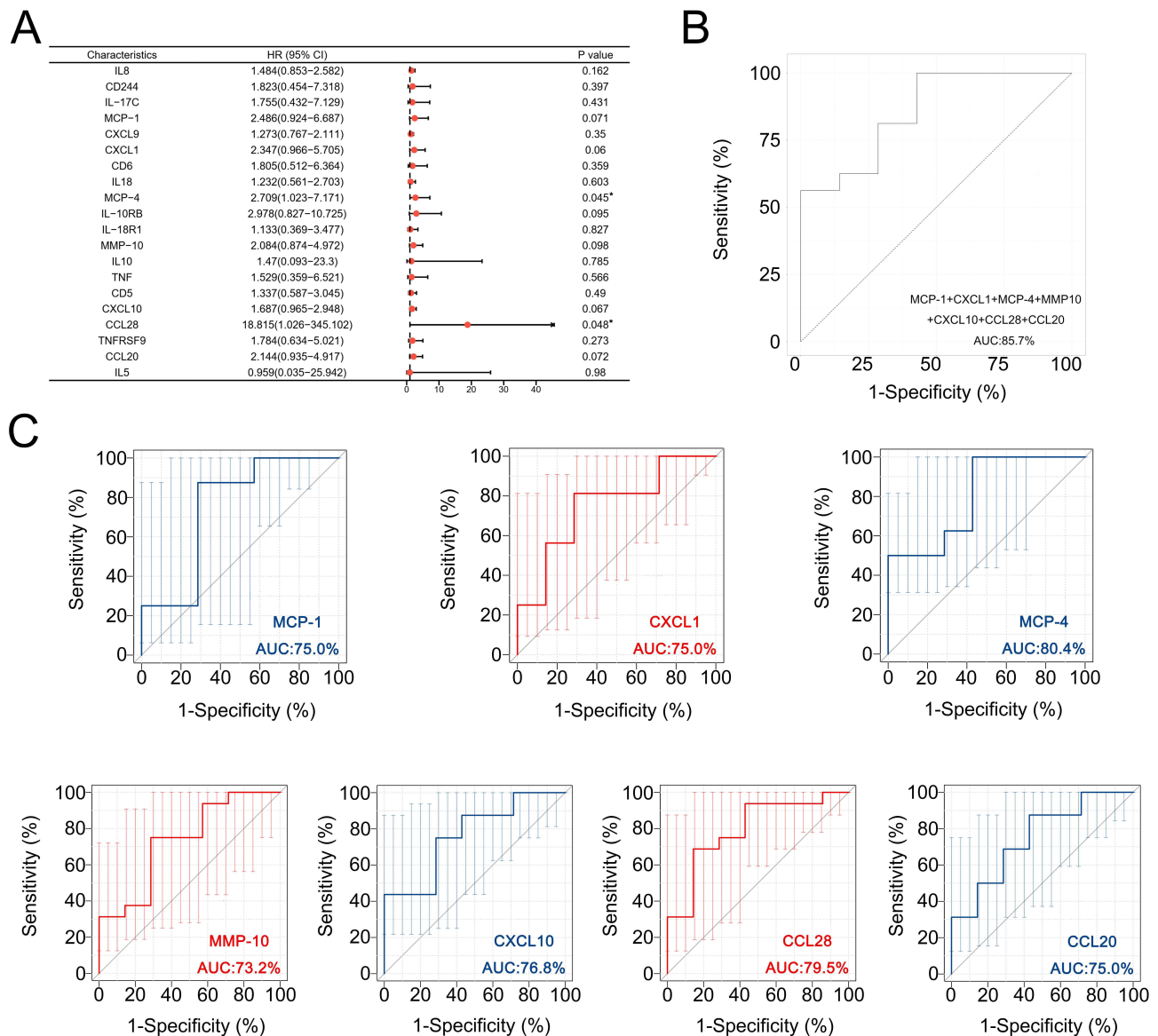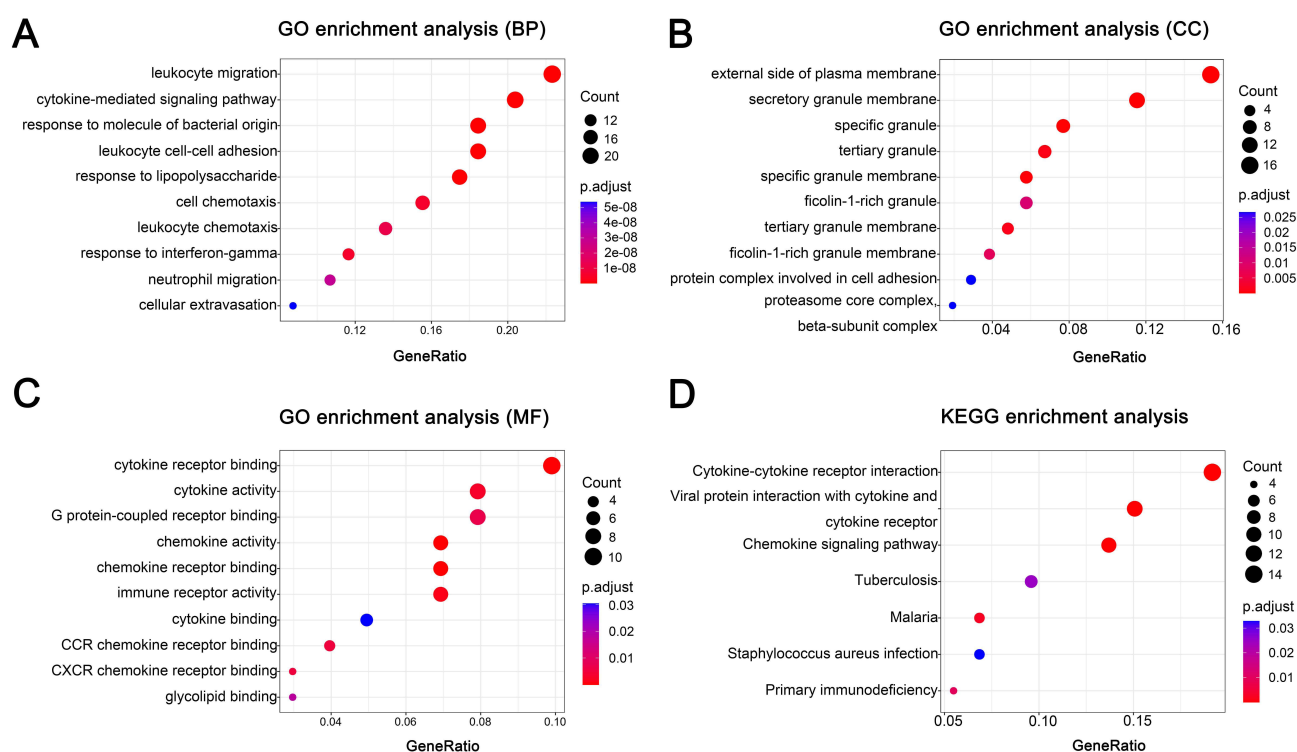
Figure 6 Predictive value of DEPs for severe GBS. (**A**) Forest plot of a one-way logistic regression analysis comparing the GBS groups with severe and mild cases. (**B**) Diagnostic ROC curve analysis of groups with mild and severe GBS; the figure displays the ROC curves of seven proteins for the combined diagnosis of severe GBS with an AUC > 0.7. (**C**) Seven proteins' ROC curves: MCP-1, CXCL1, MCP-4, MMP-10, CXCL10, CCL28, and CCL20. *P<0.05.

a substantial upregulation of MCP-1 and CXCL9 at the mRNA and protein levels. The involvement of MCP-1 and CXCL9 in GBS was further reinforced by the findings that overlapped across proteomics and genomes.

We compared two data sets, DEGs and DEPs, using GO and KEGG functional enrichment pathways in order to better explore the possible roles of DEGs. Cell chemotaxis, neutrophil migration, cellular reactions to lipopolysaccharide and bacterial-derived compounds, and leukocyte chemotaxis were all found to exhibit co-enrichment of biological processes (Figure 8A). The lumen of tertiary granules, which is the outer side of the plasma membrane, showed co-enriched cellular components (Figure 8B). This could indicate that inflammatory substances were secreted into the extracellular microenvironment. G protein-coupled receptor binding, cytokine and chemokine activity and receptor binding, and CXCR and CCR chemokine receptor binding were all found to have co-enriched molecular functions (Figure 8C). Co-enrichment involving chemokine signaling pathways, interactions between cytokines and their receptors, and interactions of viral proteins with cytokines and their receptors was

A   Volcano plot

B   Venn Plot
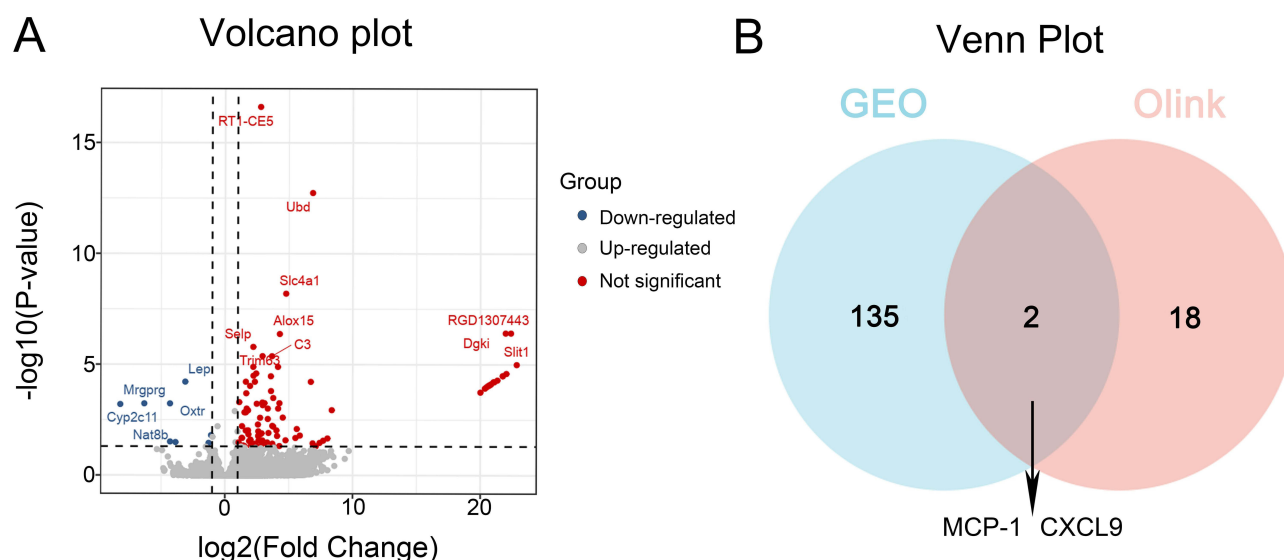
Figure 7 Genes that are expressed differently in the GEO data. (**A**) A volcano map demonstrates how peak EAN and controls have different gene expression patterns. Genes with considerably elevated expression are shown in red, genes with significantly downregulated expression are shown in blue, and genes with no differential expression are shown in grey. Each dot represents an identified gene. (**B**) Venn diagram displaying the percentage of overlapped expression between 20 DEPs tested using Olink proteomics and 137 DEGs from the rat EAN model in the GEO database.

A   GO enrichment analysis (BP)

B   GO enrichment analysis (CC)

C   GO enrichment analysis (MF)

D   KEGG enrichment analysis

Figure 8 DEGs' KEGG enrichment analysis and GO analysis. (**A**–**C**) Bubble plots showing the (BP) biological processes, (CC) cellular component biological processes, and (MF) molecular functions associated with differentially expressed proteins. (**D**) Bubble plots that display the paths that were enriched and analyzed. Horizontal coordinates show the number of genes or the total number of enriched genes, whereas vertical coordinates show enhanced biological activities or pathways. The size of the dots in the graph, which correspond to the number of genes, and their color show the p-value.

found by KEGG enrichment analysis (Figure 8D). Given that these pathways overlap, it is possible that the transcript-protein level of the inflammatory mechanism of GBS is somewhat conserved. Future research on the precise pathways must be conducted in conjunction with in vivo models.

Discussion

Guillain-Barré syndrome's pathophysiology includes intricate humoral and cellular immunological responses,[30,31] and diagnosis and treatment are complicated by the syndrome's heterogeneity.[32] By using Olink proteomics technology and increasing the sample size (n=37) in comparison to a prior work that relied on tandem mass spectrometry labeling technology (n=20),[9] we were able to obtain more accurate and sensitive detection results. As cerebrospinal fluid samples better indicate inflammatory alterations in the nerve roots, we employed them instead of serological tests of GBS.[33] Thus, the proteomic characterization of CSF inflammation during the acute phase of GBS was the main focus of our investigation. Although several molecules, including TNF, CCL20, IL8, MCP-1, IL10, and IL5, were identified as potential biological indicators, their pathogenesis and specificity must be confirmed before they can be used in clinical settings.

Certain chemokines increased expression in GBS. For the first time in our investigation, we found that CCL20 was higher in GBS CSF, positively connected with hospital stay duration (r=0.46), and showed some diagnostic utility in predicting GBS (AUC=0.75). By attracting Th17 cells, CCL20, a ligand for CCR6, may contribute to the autoimmune assault on peripheral neurons in GBS.[34–36] In multiple sclerosis (MS), plasma CCL20 correlates exponentially with disease severity, whereas the Th17 pathway is more involved in CNS demyelination in MS.[37] This variation in inflammatory location could account for a portion of CCL20's specificity in GBS. In line with other findings, we discovered increased levels of IL8, MCP-1, and CXCL10 in the CSF of GBS.[38–40] It was discovered that the degree of nerve root inflammation was reflected in the amount of IL8 in the CSF of GBS patients. In order to distinguish GBS from chronic inflammatory demyelinating polyneuropathy (CIDP), a threshold of 73 ng/L for IL8 was established, indicating that IL8 might be a molecule unique to GBS.[38] We discovered that CCR2+ monocyte/macrophage infiltration was markedly elevated in the sciatic nerve and that MCP-1 transcript levels were up in peripheral nerve tissue from EAN rats.[41] This discovery implies that monocyte recruitment in GBS peripheral nerves may be mediated via the MCP-1/CCR2 axis. Future research must use in vivo tests to further examine the specificity of chemokines in GBS, as they are seen in a wide range of inflammatory illnesses.

Huang et al discovered that TNF expression was considerably higher in serum from GBS patients and dropped following immunotherapy,[42,43] indicating that it might be connected to how GBS progresses. Notably, serum TNF may mainly originate from systemic immune activation, whereas elevated CSF TNF is more directly indicative of a localized inflammatory microenvironment in peripheral nerves. According to related research, autoimmune demyelination is triggered by the interferon gamma-induced macrophage TNF-α signaling axis, which promotes pro-inflammatory polarization through metabolic reprogramming.[44] When it comes to autoimmunity caused by Clostridium jejuni, IL10 plays a negative regulatory effect.[45] IL10 mRNA was expressed at its highest level in EAN at the peak of disease,[46] which is consistent with our observation in GBS. One possible explanation for IL10 overexpression is a compensatory anti-inflammatory response.[47] By inhibiting immunoinflammation and neural demyelination and activating the JAK-STAT pathway, IL-5 lessens the severity of EAN.[48,49] In this study, IL5 expression was reduced, and its anti-inflammatory properties might be inhibited during the acute stage of GBS. It has been proposed that IL5 facilitates the recovery of heart failure following myocardial infarction by encouraging macrophage polarization.[50] We hypothesized that IL5 expression is temporally dynamic and may be elevated during the recovery phase. Interfering with IL5 may be a viable treatment strategy for GBS, although long-term research is required to confirm this hypothesis. Furthermore, the cellular origin of IL5 and IL10 remains unclear and requires additional elucidation using flow cytometry or single-cell sequencing.

DEPs were found to be enriched in immune-related and inflammatory pathways. The TNF signaling pathway was found to be consistent with earlier research and may be involved in the regulation of the local neural immune microenvironment and promote the release of inflammatory factors by activating the macrophage NF-κB pathway.[44] The viral protein-cytokine interaction pathway's enrichment could be a sign of a molecular mimicry mechanism that was started by infections (like Campylobacter jejuni) before GBS developed. Th17 cell involvement in GBS is supported by IL17 pathway enrichment.[51,52] Unlike in MS, IL17 may target Schwann cells instead of oligodendrocytes to cause peripheral nerve demyelination in GBS.[53] But more proof is needed for this conjecture.

In our study, correlation analysis showed that differentially expressed proteins were linked with total CSF protein, IgG, IgM, neutrophil percentage, and SII. This implies that these might be clinical variables associated with inflammation in GBS.

However, both protein expression and clinical symptoms may be impacted by confounding factors such as patient age and length of disease.[54] Variations in the expression of specific differentially expressed proteins could be the cause of inflammation associated with the disease or one of the factors contributing to GBS. Therefore, this study focuses on the discovery phase to provide evidence of a preliminary association. Follow-up studies are needed to further validate the causal relationship by investigating the pathological mechanisms through in vivo experiments. CCL20 and IL5 were identified as possible independent predictors for the diagnosis of GBS through the stepwise screening of differentially expressed proteins using LASSO regression and the development of a logistic regression model.[55,56] The severity of GBS was predicted by seven DEPs: MCP-1, CXCL1, MCP-4, MMP-10, CXCL10, CCL28, and CCL20. In exploratory investigations, these biomarkers demonstrated a modest level of diagnostic effectiveness; nonetheless, multi-step validation is necessary for clinical translation. The present study provides preliminary evidence for this process.

This study has some limitations. First, because the disease is rare, the recruiting period was brief, and the sampling was intrusive (such as collecting CSF fluid), the study's sample size was small. The statistical efficacy of a small number of differentially expressed proteins was not good. Second, the AUC values of the identified biomarkers suggest some diagnostic potential; however, further, larger, prospective GBS clinical cohort investigations are required to determine their clinical relevance. Third, this study used bioinformatics analysis to suggest key signaling pathways, but there was no in vitro validation or animal experimentation. Therefore, the biological significance of these molecules and their causal relationship with GBS remain speculative, and subsequent construction of animal models of GBS is needed to validate the specific mechanisms of the identified biomarkers.

Conclusion

We concluded by identifying 20 DEPs as possible biomarkers for the diagnosis of GBS, including TNF, CCL20, IL8, MCP-1, IL10, and IL5. The chemokine signaling route, the IL17 signaling pathway, and cytokine-receptor interactions were among the pathways in which these DEPs were enriched. Although the specific mechanisms of these DEPs in GBS need to be further investigated, this study provides new clues for the clinical diagnosis of GBS. Future studies will further evaluate the diagnostic accuracy of these DEPs and their potential in clinical applications by expanding the clinical sample size and in vivo experiments.

Acknowledgments

We thank the patients and their families who participated in this study.

Author Contributions

All authors made a significant contribution to the work reported, whether that is in the conception, study design, execution, acquisition of data, analysis and interpretation, or in all these areas; took part in drafting, revising or critically reviewing the article; gave final approval of the version to be published; have agreed on the journal to which the article has been submitted; and agree to be accountable for all aspects of the work.

Funding

Disclosure

The authors have declared that no competing interest exists in this work.

References

1. Shahrizaila N, Lehmann HC, Kuwabara S. Guillain-Barré syndrome. *Lancet*. 2021;397(10280):1214–1228. doi:10.1016/S0140-6736(21)00517-1
2. Florian IA, Lupan I, Sur L, Samasca G, Timiş TL. To be, or not to be… Guillain-Barré syndrome review. *Autoimmun Rev*. 2021;20(12):28.
3. Darweesh SK, Polinder S, Mulder MJ, et al. Health-related quality of life in Guillain-Barré syndrome patients: a systematic review. *J Peripher Nerv Syst*. 2014;19(1):24–35. doi:10.1111/jns5.12051
4. Willison HJ, Jacobs BC, van Doorn PA. Guillain-Barré syndrome. *Lancet*. 2016;388(10045):717–727. doi:10.1016/S0140-6736(16)00339-1

 6715

5. Laman JD, Huizinga R, Boons GJ, Jacobs BC. Guillain-Barré syndrome: expanding the concept of molecular mimicry. *Trends Immunol*. 2022;43 (4):296–308. doi:10.1016/j.it.2022.02.003

6. Li X, Yang L, Wang G, et al. Extensive cytokine biomarker analysis in serum of Guillain-Barré syndrome patients. *Sci Rep*. 2023;13(1):023–35610.

7. Liu S, Dong C, Ubogu EE. Immunotherapy of Guillain-Barré syndrome. *Hum Vaccin Immunother*. 2018;14(11):2568–2579. doi:10.1080/21645515.2018.1493415

8. Breville G, Sukockiene E, Vargas MI, Lascano AM. Emerging biomarkers to predict clinical outcomes in Guillain-Barré syndrome. *Expert Rev Neurother*. 2023;23(12):1201–1215. doi:10.1080/14737175.2023.2273386

9. Ding Y, Shi Y, Wang L, et al. Potential biomarkers identified by tandem mass tags based quantitative proteomics for diagnosis and classification of Guillain-Barré syndrome. *Eur J Neurol*. 2022;29(4):1155–1164. doi:10.1111/ene.15213

10. Min YG, Ju W, Seo JW, et al. Serum C3 complement levels predict prognosis and monitor disease activity in Guillain-Barré syndrome. *J Neurol Sci*. 2023;444(120512):28. doi:10.1016/j.jns.2022.120512

11. Thomma RCM, Fokke C, Walgaard C, et al. High and persistent anti-gm1 antibody titers are associated with poor clinical recovery in Guillain-Barré syndrome. *Neurol Neuroimmunol Neuroinflamm*. 2023;10(4). doi:10.1212/NXI.0000000000200107

12. Oeztuerk M, Henes A, Schroeter CB, et al. Current biomarker strategies in autoimmune neuromuscular diseases. *Cells*. 2023;12(20):2456. doi:10.3390/cells12202456

13. Wik L, Nordberg N, Broberg J, et al. Proximity extension assay in combination with next-generation sequencing for high-throughput proteome-wide analysis. *Mol Cell Proteomics*. 2021;20(100168):27. doi:10.1016/j.mcpro.2021.100168

14. Topol EJ. The revolution in high-throughput proteomics and AI. *Science*. 2024;385(6716):26. doi:10.1126/science.ads5749

15. Sun BB, Chiou J, Traylor M, et al. Plasma proteomic associations with genetics and health in the UK biobank. *Nature*. 2023;622(7982):329–338. doi:10.1038/s41586-023-06592-6

16. Fokke C, van den Berg B, Drenthen J, Walgaard C, van Doorn PA, Jacobs BC. Diagnosis of Guillain-Barré syndrome and validation of brighton criteria. *Brain*. 2014;137(Pt 1):33–43. doi:10.1093/brain/awt285

17. Joseph N, Shrigiri S. Predictors of treatment outcome and clinical profile among Guillain- Barre syndrome patients in South India. *Rev Recent Clin Trials*. 2023;18(4):258–268. doi:10.2174/0115748871254419231019053136

18. Hughes RA, Newsom-Davis JM, Perkin GD, Pierce JM. Controlled trial prednisolone in acute polyneuropathy. *Lancet*. 1978;2(8093):750–753. doi:10.1016/S0140-6736(78)92644-2

19. Assarsson E, Lundberg M, Holmquist G, et al. Homogenous 96-plex PEA immunoassay exhibiting high sensitivity, specificity, and excellent scalability. *PLoS One*. 2014;9(4):e95192. doi:10.1371/journal.pone.0095192

20. Bao XH, Chen BF, Liu J, et al. Olink proteomics profiling platform reveals non-invasive inflammatory related protein biomarkers in autism spectrum disorder. *Front Mol Neurosci*. 2023;16(1185021). doi:10.3389/fnmol.2023.1185021

21. Wang X, Yip KC, He A, et al. Plasma olink proteomics identifies CCL20 as a novel predictive and diagnostic inflammatory marker for preeclampsia. *J Proteome Res*. 2022;21(12):2998–3006. doi:10.1021/acs.jproteome.2c00544

22. Kanehisa M, Goto S. KEGG: kyoto encyclopedia of genes and genomes. *Nucleic Acids Res*. 2000;28(1):27–30. doi:10.1093/nar/28.1.27

23. Gene Ontology C. Gene ontology consortium: going forward. *Nucleic Acids Res*. 2015;43(Database issue):26.

24. Subramanian A, Tamayo P, Mootha VK, et al. Gene set enrichment analysis: a knowledge-based approach for interpreting genome-wide expression profiles. *Proc Natl Acad Sci U S A*. 2005;102(43):15545–15550. doi:10.1073/pnas.0506580102

25. Szklarczyk D, Gable AL, Lyon D, et al. STRING v11: protein-protein association networks with increased coverage, supporting functional discovery in genome-wide experimental datasets. *Nucleic Acids Res*. 2019;47(D1):D607–D613. doi:10.1093/nar/gky1131

26. Han YH, Ma DY, Lee SJ, et al. Bioinformatics analysis of novel targets for treating cervical cancer by immunotherapy based on immune escape. *Cancer Genomics Proteomics*. 2023;20(4):383–397. doi:10.21873/cgp.20390

27. Wang H, Zhang L, Liu Z, et al. Predicting medication nonadherence risk in a Chinese inflammatory rheumatic disease population: development and assessment of a new predictive nomogram. *Patient Prefer Adherence*. 2018;12:1757–1765. doi:10.2147/PPA.S159293

28. Song Y, Liu S, Qiu W, Liu K, Zhang HL. Prediction of mechanical ventilation in Guillain-Barré syndrome at admission: construction of a nomogram and comparison with the EGRIS model. *Heliyon*. 2024;10(9):15.

29. Lätti S, Niinivehmas S, Pentikäinen OT. Rocker: open source, easy-to-use tool for AUC and enrichment calculations and ROC visualization. *J Cheminform*. 2016;8(1):016–0158. doi:10.1186/s13321-016-0158-y

30. Shastri A, Al Aiyan A, Kishore U, Farrugia ME. Immune-mediated neuropathies: pathophysiology and management. *Int J Mol Sci*. 2023;24(8). doi:10.3390/ijms24087288

31. van Doorn PA, Ruts L, Jacobs BC. Clinical features, pathogenesis, and treatment of Guillain-Barré syndrome. *Lancet Neurol*. 2008;7(10):939–950. doi:10.1016/S1474-4422(08)70215-1

32. Sun T, Chen X, Shi S, Liu Q, Cheng Y. Peripheral blood and cerebrospinal fluid cytokine levels in Guillain Barré syndrome: a systematic review and meta-analysis. *Front Neurosci*. 2019;13:717. eCollection 2019. doi:10.3389/fnins.2019.00717

33. Li YJ, Zhang XY, Zhang WJ, et al. Proteomics analysis of immune response-related proteins in Guillain-Barré syndrome (GBS) and chronic inflammatory demyelinating polyneuropathy (CIDP). *J Neuroimmunol*. 2024;394(578423):30. doi:10.1016/j.jneuroim.2024.578423

34. Meitei HT, Jadhav N, Lal G. CCR6-CCL20 axis as a therapeutic target for autoimmune diseases. *Autoimmun Rev*. 2021;20(7):7. doi:10.1016/j.autrev.2021.102846

35. Martina MG, Giorgio C, Allodi M, et al. Discovery of small-molecules targeting the CCL20/CCR6 axis as first-in-class inhibitors for inflammatory bowel diseases. *Eur J Med Chem*. 2022;243(114703):29. doi:10.1016/j.ejmech.2022.114703

36. Ye C, Guo X, Wu J, Wang M, Ding H, Ren X. CCL20/CCR6 mediated macrophage activation and polarization can promote adenoid epithelial inflammation in adenoid hypertrophy. *J Inflamm Res*. 2022;15:6843–6855. doi:10.2147/JIR.S390210

37. Huang J, Khademi M, Fugger L, et al. Inflammation-related plasma and CSF biomarkers for multiple sclerosis. *Proc Natl Acad Sci U S A*. 2020;117 (23):12952–12960. doi:10.1073/pnas.1912839117

38. Kmezic I, Gustafsson R, Fink K, et al. Validation of elevated levels of interleukin-8 in the cerebrospinal fluid, and discovery of new biomarkers in patients with GBS and CIDP using a proximity extension assay. *Front Immunol*. 2023;14(1241199). doi:10.3389/fimmu.2023.1241199

39. Chiang S, Ubogu EE. The role of chemokines in Guillain-Barré syndrome. *Muscle Nerve*. 2013;48(3):320–330.

40. Press R, Pashenkov M, Jin JP, Link H. Aberrated levels of cerebrospinal fluid chemokines in Guillain-Barré syndrome and chronic inflammatory demyelinating polyradiculoneuropathy. *J Clin Immunol*. 2003;23(4):259–267. doi:10.1023/A:1024532715775

41. Orlikowski D, Chazaud B, Plonquet A, et al. Monocyte chemoattractant protein 1 and chemokine receptor CCR2 productions in Guillain-Barré syndrome and experimental autoimmune neuritis. *J Neuroimmunol*. 2003;134(1–2):118–127. doi:10.1016/S0165-5728(02)00393-4

42. Huang P, Xu M, He XY. Correlations between microRNA-146a and immunoglobulin and inflammatory factors in Guillain-Barré syndrome. *J Int Med Res*. 2020;48(3):0300060520904842. doi:10.1177/0300060520904842

43. Lv L, Xu H, Zhang H, Qi Q. Clinical efficacy of high-dose intravenous gammaglobulin in acute Guillain-Barre syndrome and effect on serum concentration of inflammatory factors. *Am J Transl Res*. 2022;14(9):6295–6302.

44. Wang Y, Guo L, Yin X, et al. Pathogenic TNF-α drives peripheral nerve inflammation in an Aire-deficient model of autoimmunity. *Proc Natl Acad Sci U S A*. 2022;119(4):2114406119. doi:10.1073/pnas.2114406119

45. Malik A, Brudvig JM, Gadsden BJ, Ethridge AD, Mansfield LS. Campylobacter jejuni induces autoimmune peripheral neuropathy via Sialoadhesin and Interleukin-4 axes. *Microbes*. 2022;14(1):2064706.

46. Uchi T, Konno S, Kihara H, Fujioka T. Siponimod ameliorates experimental autoimmune neuritis. *J Neuroinflammation*. 2023;20(1):023–02706. doi:10.1186/s12974-023-02706-z

47. Hayat S, Asad A, Munni MA, et al. Interleukin-10 promoter polymorphisms and haplotypes in patients with Guillain-Barré syndrome. *Ann Clin Transl Neurol*. 2023;13(10):51939.

48. Dougan M, Dranoff G, Dougan SK. GM-CSF, IL-3, and IL-5 family of cytokines: regulators of inflammation. *Immunity*. 2019;50(4):796–811. doi:10.1016/j.immuni.2019.03.022

49. Tran GT, Hodgkinson SJ, Carter NM, et al. IL-5 promotes induction of antigen-specific CD4+CD25+ T regulatory cells that suppress autoimmunity. *Blood*. 2012;119(19):4441–4450. doi:10.1182/blood-2011-12-396101

50. Xu JY, Xiong YY, Tang RJ, et al. Interleukin-5-induced eosinophil population improves cardiac function after myocardial infarction. *Cardiovasc Res*. 2022;118(9):2165–2178. doi:10.1093/cvr/cvab237

51. Xie Y, Han R, Li Y, et al. P2X7 receptor antagonists modulate experimental autoimmune neuritis via regulation of NLRP3 inflammasome activation and Th17 and Th1 cell differentiation. *J Neuroinflammation*. 2024;21(1):024–03057. doi:10.1186/s12974-024-03057-z

52. Debnath M, Nagappa M, Dutta D, et al. Evidence of altered Th17 pathway signatures in the cerebrospinal fluid of patients with Guillain Barré syndrome. *J Clin Neurosci*. 2020;75:176–180. doi:10.1016/j.jocn.2020.03.010

53. Debnath M, Nagappa M, Murari G, Taly AB. IL-23/IL-17 immune axis in Guillain Barré Syndrome: exploring newer vistas for understanding pathobiology and therapeutic implications. *Cytokine*. 2018;103:77–82. doi:10.1016/j.cyto.2017.12.029

54. Hegen H, Ladstätter F, Bsteh G, et al. Cerebrospinal fluid protein in Guillain-Barré syndrome: need for age-dependent interpretation. *Eur J Neurol*. 2021;28(3):965–973. doi:10.1111/ene.14600

55. Ning P, Yang B, Yang X, et al. A nomogram to predict mechanical ventilation in Guillain-Barré syndrome patients. *Acta Neurol Scand*. 2020;142(5):466–474. doi:10.1111/ane.13294

56. Di X, Wang J, Li L, Liu L. Establishment of a single-center-based early prognostic scoring system for Guillain-Barré syndrome. *BMC Neurol*. 2023;23(1):023–03143. doi:10.1186/s12883-023-03143-4